Bioorganic Chemistry xxx (xxxx) xxxx

Contents lists available at ScienceDirect

Bioorganic Chemistry

journal homepage: www.elsevier.com/locate/bioorg

# ω-Quinazolinonylalkyl aryl ureas as reversible inhibitors of monoacylglycerol lipase

Florian M. Dato[a,b], Jörg-Martin Neudörfl[b], Michael Gütschow[c], Bernd Goldfuss[b,*], Markus Pietsch[a,*]

[a] Institute II of Pharmacology, Center of Pharmacology, Medical Faculty, University of Cologne, Gleueler Strasse 24, 50931 Cologne, Germany
[b] Institute of Organic Chemistry, Department of Chemistry, University of Cologne, Greinstrasse 4, 50939 Cologne, Germany
[c] Pharmaceutical Institute, Pharmaceutical Chemistry I, University of Bonn, An der Immenburg 4, 53121 Bonn, Germany

ARTICLE INFO

*Keywords:*
Serine hydrolases
Cholesterol esterase
Monoacylglycerol lipase
Fatty acid amide hydrolase
Inhibitors
Promiscuous inhibition
Enzyme kinetics

ABSTRACT

The serine hydrolase monoacylglycerol lipase (MAGL) is involved in a plethora of pathological conditions, in particular pain and inflammation, various types of cancer, metabolic, neurological and cardiovascular disorders, and is therefore a promising target for drug development. Although a large number of irreversible-acting MAGL inhibitors have been discovered over the past years, there are only few compounds known so far which inhibit the enzyme in a reversible manner. Therefore, much effort is put into the development of novel chemical entities showing reversible inhibitory behavior, which is thought to cause less undesired side effects. To explore a wide range of chemical structures as MAGL binders, we have applied a virtual screening approach by docking small molecules into the crystal structure of human MAGL (hMAGL) and envisaged a library of 45 selected compounds which were then synthesized. Biochemical investigations included the determination of the inhibitory potency on hMAGL and two related hydrolases, i.e. human fatty acid amide hydrolase (hFAAH) and murine cholesterol esterase (mCEase). The most promising candidates from theses analyses, i.e. three ω-quinazolinonylalkyl aryl ureas bearing alkyl spacers of three to five methylene groups, exhibited $IC_{50}$ values of 20–41 μM and reversible, detergent-insensitive behavior towards hMAGL. Among these compounds, the inhibitor 1-(3,5-bis(trifluoromethyl)phenyl)-3-(4-(4-oxo-3,4-dihydroquinazolin-2-yl)butyl)urea (**96**) was selected for further kinetic characterization, yielding a dissociation constant $K_i$ = 15.4 μM and a mixed-type inhibition with a pronounced competitive component (α = 8.94). This mode of inhibition was further supported by a docking experiment, which suggested that the inhibitor occupies the substrate binding pocket of hMAGL.

## 1. Introduction

The serine hydrolase monoacylglycerol lipase (MAGL, EC 3.1.1.23) is part of the endocannabinoid system and has been found in both the central nervous system and peripheral tissues, including liver, kidneys, testis, lung, prostate and small intestine [1–4]. MAGL is important for the regulation of a vast number of different pathological processes, particularly cancer, but also inflammation and pain, metabolic, neurological, and cardiovascular disorders [5–17]. In aggressive human cancer cells (e.g. breast, ovarian, colorectal, melanoma, liver and prostate), for example, MAGL is highly expressed [4,5,18,19] and acts as a key metabolic hub "regulating a fatty acid network enriched in pro-tumorigenic lipids" [20]. These signaling lipids promote the survival, the migration, invasion and growth of cancer cells. In case of aggressive prostate cancer cells, MAGL also suppresses anti-tumorigenic endocannabinoid signals [4,5,12,13,21]. Knocking down MAGL or blocking its activity by the irreversible carbamate inhibitor JZL 184 (**108**, Fig. 1) were shown to result in a reduced tumor growth rate and a decreased cancer cell migration accompanied by a lower conversion of monoacylglycerols to pro-tumorigenic signal lipids [4,5,21]. However, complete inhibition of MAGL results in a functional antagonism of the cerebral cannabinoid receptor CB1, and, thus, might be associated with psychiatric side effects [22]. These side effects might be prevented by using reversibly acting MAGL inhibitors [15,22]; however, the superiority of such compounds over irreversible enzyme modifiers will have to be proven by future studies [23].

* Corresponding authors at: Institute II of Pharmacology, Center of Pharmacology, Medical Faculty, University of Cologne, Gleueler Str. 24, D-50931 Cologne, Germany. (Markus Pietsch). Institute of Organic Chemistry, Department of Chemistry, University of Cologne, Greinstr. 4, D-50939 Cologne, Germany. (Bernd Golfuss).
*E-mail addresses:* goldfuss@uni-koeln.de (B. Goldfuss), markus.pietsch@uk-koeln.de (M. Pietsch).

https://doi.org/10.1016/j.bioorg.2019.103352
Received 16 August 2019; Received in revised form 2 October 2019; Accepted 9 October 2019

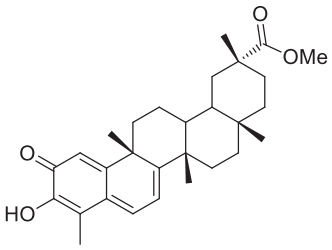

pristimerin (**1**)
$IC_{50}$ = 0.093 μM

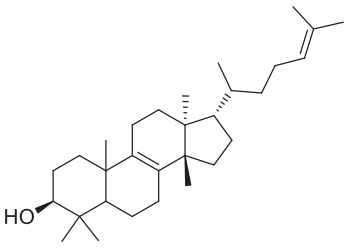

euphenol (**2**)
$IC_{50}$ = 0.315 μM

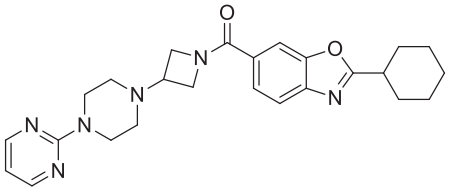

ZYH (**3**)
$IC_{50}$ = 0.010 μM

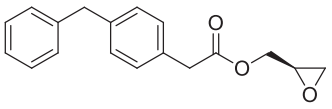

**4**
$K_i$ = 40 μM

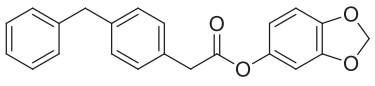

**5**
$K_i$ = 0.40 μM

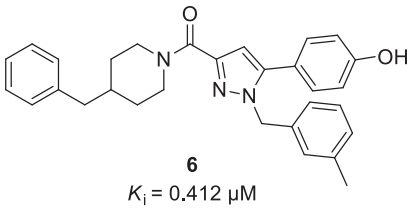

**6**
$K_i$ = 0.412 μM

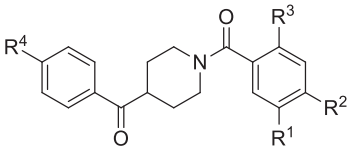

**7-9**

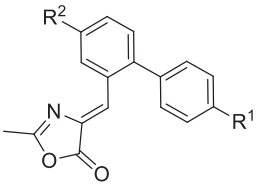

**10**, **11**

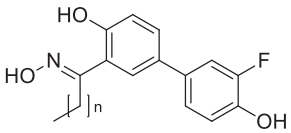

**12**, **13**

**7**: $R^1$ = H; $R^2$ = $OCH_3$; $R^3$ = H; $R^4$ = Cl; $K_i$ = 8.6 μM
**8**: $R^1$ = OH; $R^2$ = H; $R^3$ = H; $R^4$ = Cl; $K_i$ = 0.65 μM
**9**: $R^1$ = OH; $R^2$ = H; $R^3$ = F; $R^4$ = *i*-Pr; $K_i$ = 0.039 μM

**10**: $R^1$ = F; $R^2$ = H; $IC_{50}$ = 1.6 μM
**11**: $R^1$ = $OCH_3$; $R^2$ = 4-$OCH_3$-$C_6H_4$; $IC_{50}$ = 0.35 μM
**12**: n = 10; $IC_{50}$ = 0.71 μM
**13**: n = 12; $IC_{50}$ = 0.68 μM

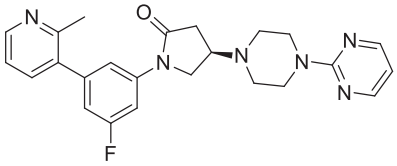

**14**
$IC_{50}$ = 0.0036 μM

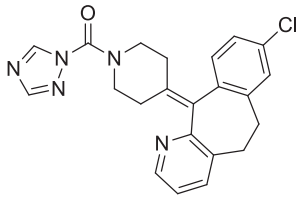

**15**
$IC_{50}$ = 0.046 μM

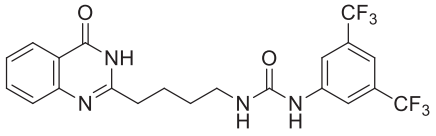

**96**
$K_i$ = 15.4 μM

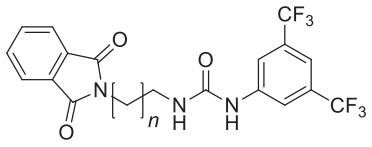

**106**, **107**

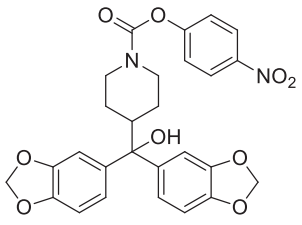

**106**: n = 2; inhibition: 35.9% at [I] = 25 μM
**107**: n = 3; inhibition: 31.5% at [I] = 25 μM

JZL 184 (**108**)
$IC_{50}$ = 0.314 μM

**Fig. 1.** A selection of reported reversible inhibitors of rat (**1**, **2**, **5**) and human (**3**, **4**, **6–15**) MAGL. In this study, quinazolinone **96** was investigated on human MAGL, with ω-phthalimidoalkyl 3,5-bis(trifluoromethyl)phenyl ureas **106** and **107** as well as irreversibly acting carbamate JZL 184 (**1 0 8)** being used as reference inhibitors [43].

In recent years, a plethora of MAGL inhibitors have been published often containing reactive carbamate or urea moieties, which lead to an irreversible inactivation of the enzyme by covalent modification of the active serine residue [12,23–26]. In contrast, only few reversibly acting MAGL inhibitors are known so far [23,24] and, thus, "novel chemical classes displaying a reversible mechanism of action" towards this

enzyme [23] are much-needed. Examples of reversible MAGL inhibitors (Fig. 1) include the steroids pristimerin (**1**) and euphenol (**2**), which have been identified by screening a commercially available compound library [27]. Furthermore, the piperazinyl azetidinyl amide ZYH (**3**) developed by Janssen Pharmaceutica [28] was the first reversible inhibitor co-crystallized with MAGL (PDB: 3PE6) [29]. Many efforts in investigating reversibly acting compounds have also been made by the groups of Lopez-Rodríguez and Tuccinardi, who identified, for example, the 4-benzylphenylacetyl esters **4** [30] and **5** [31], the *N*-acyl piperidines **6** and **7–9**, [32–35], and the biphenyl derivatives **10–13** [36–38]. In addition, Aida et al. [39] discovered the piperazinyl pyrrolidin-2-one **14** and Patel et al. [40] described the loratadine analogue **15** as novel MAGL inhibitors exhibiting reversible behavior.

The objective of our study was the identification of novel chemical entities reversibly acting on human MAGL (hMAGL) as potent and selective inhibitors. For this purpose, we initially applied an *in silico* approach by virtual screening of low molecular weight compounds (among others, structures from the ZINC database) [41,42] using molecular docking on the crystal structure of hMAGL (PDB: 3PE6). A selection of identified *in silico* hits was then synthesized and characterized in terms of its inhibitory activity on hMAGL. To investigate the selectivity of inhibitors for MAGL over other serine hydrolases, all compounds were also assayed on human fatty acid amide hydrolase (hFAAH, EC 3.5.1.99) and murine cholesterol esterase (mCEase, EC 3.1.1.13), both of which accept fatty acid derivatives as physiological substrates similar to MAGL. Those inhibitors most active on the three serine hydrolases were re-tested in the presence of Triton X-100 (0.01% (v/v)) to exclude promiscuous inhibition, leaving three quinazolinones (**85**, **96** and **97**) which inhibited hMAGL with $IC_{50}$ values in the mid-micromolar range. Finally, the binding of compound **96** (Fig. 1) to hMAGL was analyzed by a detailed kinetic investigation, yielding a mixed-type mode of inhibition with a pronounced competitive component ($\alpha = 8.94$) and a $K_i$ value of 15.4 μM.

## 2. Results and discussion

### 2.1. Chemistry

We prepared a library of 45 compounds from eight substance classes, including sulfonacetamides, oxalamides, squaramides, thiazoles, quinazolinones, imidazolones, triazoles, and (oxa)naphthalenes (Schemes 1–6 and S1–S5). Representative synthetic routes to bioactive compounds are outlined below; for others, see supplementary material.

Six 2-sulfonacetamide derivatives containing either aromatic or aliphatic amide residues (Scheme 1) were synthesized starting from 1-bromo-3-phenylpropane and thioglycolic acid followed by oxidation of the resulting thioether to the corresponding sulfonyl derivative with hydrogen peroxide in glacial acetic acid to yield sulfonylacetic acid **16** in 62% yield. The carboxylic acid was then converted to the amides **17–22** (51–87%) by means of 1-ethyl-3-(3-dimethylaminopropyl)carbodiimide hydrochloride (EDC × HCl) and 1-hydroxybenzotriazole hydrate (HOBt). While 3,5-bis(trifluoromethyl)aniline and 3,5-bis (trifluoromethyl)benzylamine were obtained from commercial sources, the 3′,5′-bis(trifluoromethyl)-substituted biphenylamines **102–104** and 1-(3,5-bis(trifluoromethyl)phenyl)piperazine (**105**) (Scheme S7) were prepared as previously described by Dato et al. [43]

Synthesis of nine oxalamides with various substitution patterns (Scheme 2) started from ethyl chlorooxoacetate by reaction with various commercially available amines or previously synthesized 1-(3,5-bis (trifluoromethyl)phenyl)piperazine (**105**)[43] to obtain the respective ethyl-2-amino-2-oxoacetates **23–26** in 71–92% yield. After saponification, the free carboxylic acids **27–30** formed in 70–90% yield were then coupled with various amines, amongst them compounds **103–105**, yielding the target compounds **31–39** (23–85%). The molecular structure of oxalamide **37** was proven by X-ray crystallography (Fig. S17).

To obtain the three squaramides **42–44** (38–72%, Scheme 3), 3,4-diethoxy-3-cyclobutene-1,2-dione was initially treated with 3,5-bis (trifluoromethyl)aniline and 3′,5′-bis(trifluoromethyl)-[1,1′-biphenyl]-4-amine (**104**) to obtain the anilides **40** (72%) and **41** (93%), respectively, which were then reacted with the aliphatic amines 3-phenylpropylamine and 2-(4-phenylpiperazin-1-yl)ethanamine (**100**, Scheme S6). Squareamides have recently drawn our attention, since derivatives of the compounds investigated herein were found to act as efficient hydrogen-bonding catalysts mediating the “enantioselective Michael addition of 4-hydroxycoumarin to β-nitrostyrenes” [44].

Thiazoles **48–51**, **55** and **56** were prepared via two different synthesis routes (Schemes 4 and S1). The synthetic route to obtain thiazoles **55** and **56** (Scheme 4) started from benzoyl chloride by reaction with thiourea and ammonium hydroxide to obtain *N*-carbamothioylbenzamide **52** (52%), which was reacted with ethyl bromopyruvate yielding thiazole **53** (94%) and subsequently saponified to the free carboxylic acid **54** (99%). Final amide coupling using 1-phenylpiperazine and 1-(3,5-bis(trifluoromethyl)phenyl)piperazine (**1 0 5**) gave the target thiazoles **55** (68%) and **56** (68%), respectively. The structures of **55** and **56** were confirmed by X-ray crystallography (Figs. S19 and S20).

Our series was further completed by imidazolones **59** and **60** (Scheme S2), triazoles **62**, **65**, **67**, **72**, **74** (Schemes S3 and S4) and (oxa)naphthalenes **75**, **77–81** (Scheme S5).

Synthesis of eight quinazolinone derivatives (Schemes 5 and 6) containing either a urea (**84–86**, **96** and **97**) or an amide moiety (**87–89**) started by preparing the quinazolinone heterocycle bearing 2-alkyl spacers of 2–5 methylene units with terminal carboxylic acid (**82**, 54%; **83**, 81%) or primary amino groups (**94**, **95**; overall yields based on **90** and **91** [43] were 53% and 62%, respectively). Then, amide coupling of the carboxylic acids with commercially available amines and 1-(3,5-bis(trifluoromethyl)phenyl)piperazine (**1 0 5**) using standard conditions (EDC × HCl, HOBt) gave the target compounds **87–89** (76–79%), whereas the urea derivatives **84–86** (8–21%) were accessible by Curtius rearrangement of the carboxylic acid azides of **82** and **83** followed by trapping of the formed isocyanates with anilines (Scheme 5). The final quinazolinones **96** (51%) and **97** (53%) resulted from the amines **94** and **95**, respectively, by reaction with 3,5-bis(trifluoromethyl)phenyl isocyanate (Scheme 6). Successful synthesis of **96**

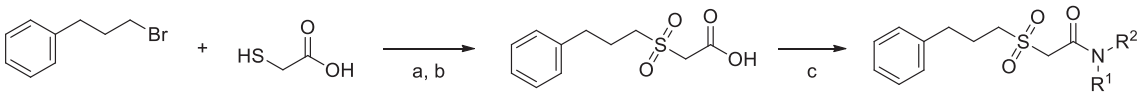


**16**

**17**: $R^1$ = H, $R^2$ = 3,5-$(CF_3)_2C_6H_3$
**18**: $R^1$ = H, $R^2$ = $CH_2$-(3,5-$(CF_3)_2C_6H_3$)
**19**: $R^1$ = H, $R^2$ = $C_6H_4$-2-(3',5'-$(CF_3)_2C_6H_3$)
**20**: $R^1$ = H, $R^2$ = $C_6H_4$-3-(3',5'-$(CF_3)_2C_6H_3$)
**21**: $R^1$ = H, $R^2$ = $C_6H_4$-4-(3',5'-$(CF_3)_2C_6H_3$)
**22**: $R^1$, $R^2$ = Pip-4-(3',5'-$(CF_3)_2C_6H_3$)

**Scheme 1.** Synthesis of 2-sulfonacetamides **17–22**. Reagents and conditions: (a) NaOH, MeOH, 14 h, RT; (b) $H_2O_2$, AcOH, 14 h, RT; (c) amine, EDC × HCl, HOBt, $CH_2Cl_2$, 14 h, 0 °C → RT. Pip, 1,4-disubstituted piperazine.

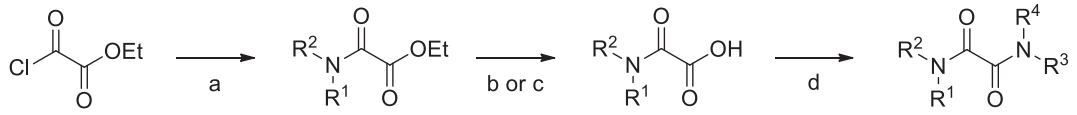


23-26 27-30 31-39

| compd | $R^1$ | $R^2$ | $R^3$ | $R^4$ |
|---|---|---|---|---|
| **23**, **27** | H | Ph | | |
| **24**, **28** | H | 3,5-$(CF_3)_2C_6H_3$ | | |
| **25**, **29** | H | $(CH_2)_3$-Ph | | |
| **26**, **30** | Pip-4-(3',5'-$(CF_3)_2C_6H_3$) | | | |
| **31** | H | Ph | Pip-4-Ph | |
| **32** | H | Ph | Pip-4-(3',5'-$(CF_3)_2C_6H_3$) | |
| **33** | H | 3,5-$(CF_3)_2C_6H_3$ | Pip-4-Ph | |
| **34** | H | 3,5-$(CF_3)_2C_6H_3$ | Pip-4-(3',5'-$(CF_3)_2C_6H_3$) | |
| **35** | Pip-4-(3',5'-$(CF_3)_2C_6H_3$) | | H | $(CH_2)_3$-Ph |
| **36** | H | 3,5-$(CF_3)_2C_6H_3$ | H | $(CH_2)_3$-Ph |
| **37** | H | $(CH_2)_3$-Ph | H | $CH_2$-(3,5-$(CF_3)_2C_6H_3$) |
| **38** | H | $(CH_2)_3$-Ph | H | $C_6H_4$-3-(3',5'-$(CF_3)_2C_6H_3$) |
| **39** | H | $(CH_2)_3$-Ph | H | $C_6H_4$-4-(3',5'-$(CF_3)_2C_6H_3$) |

**Scheme 2.** Synthesis of oxalamides **31**–**39**. Reagents and conditions: (a) amine, TEA, THF, 14 h, 0 °C → RT; (b) KOH, $H_2O$, EtOH, 2 h, 0 °C → RT; (c) LiOH, $H_2O$, THF, 2 h, 0 °C → RT; (d) amine, EDC × HCl, HOBt, $CH_2Cl_2$, 14 h, 0 °C → RT. Pip, 1,4-disubstituted piperazine.

was proven by X-ray crystallography (Fig. S22).

All intermediates and final products were structurally analyzed by $^1$H and $^{13}$C NMR spectroscopy, with the respective spectra being shown in the supplementary material (Figs. S23–S106).

### 2.2. Screening for inhibitors of hMAGL, hFAAH and mCEase

The hydrolytic activity of hMAGL, hFAAH and mCEase was determined as previously described by Dato et al. [43,45] using the chromogenic compound 4-NPB and the fluorogenic substrates D-MAP and 4-MUB, respectively. Screening for inhibition of the three enzymes by our library of 45 compounds was initially done at a concentration of 25 μM, with the residual enzymatic activities being given in Figs. S1–S7. Eight of these compounds (amongst them one 2-sulfonacetamide (**21**), two oxalamides (**32** and **34**), one squareamide (**42**), one thiazole (**56**) and three quinazolinones (**85**, **96** and **97**)) caused residual enzymatic activities ≤65% towards at least one of the hydrolases (which corresponds to a calculated $IC_{50}$ value ≤46 μM) and, thus, were selected for further investigations (Table 1).

Promiscuous behavior of the identified hits was excluded by

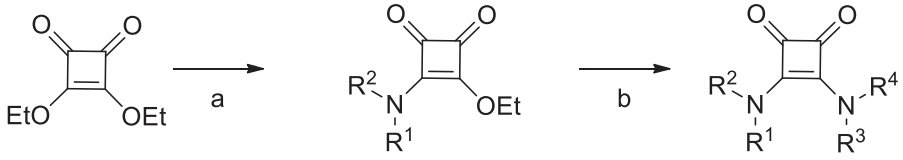


**40**, **41** **42-44**

| compd | $R^1$ | $R^2$ | $R^3$ | $R^4$ |
|---|---|---|---|---|
| **40** | H | 3,5-$(CF_3)_2C_6H_3$ | | |
| **41** | H | $C_6H_4$-4-(3',5'-$(CF_3)_2C_6H_3$) | | |
| **42** | H | 3,5-$(CF_3)_2C_6H_3$ | H | $(CH_2)_3$-Ph |
| **43** | H | $C_6H_4$-4-(3',5'-$(CF_3)_2C_6H_3$) | H | $(CH_2)_3$-Ph |
| **44** | H | $C_6H_4$-4-(3',5'-$(CF_3)_2C_6H_3$) | H | $(CH_2)_2$-Pip-4-Ph |

**Scheme 3.** Synthesis of squaramides **42**–**44**. Reagents and conditions: (a) aniline, MeOH, 48 h, RT; (b) amine, $CH_2Cl_2$, 24 h, RT. Pip, 1,4-disubstituted piperazine.

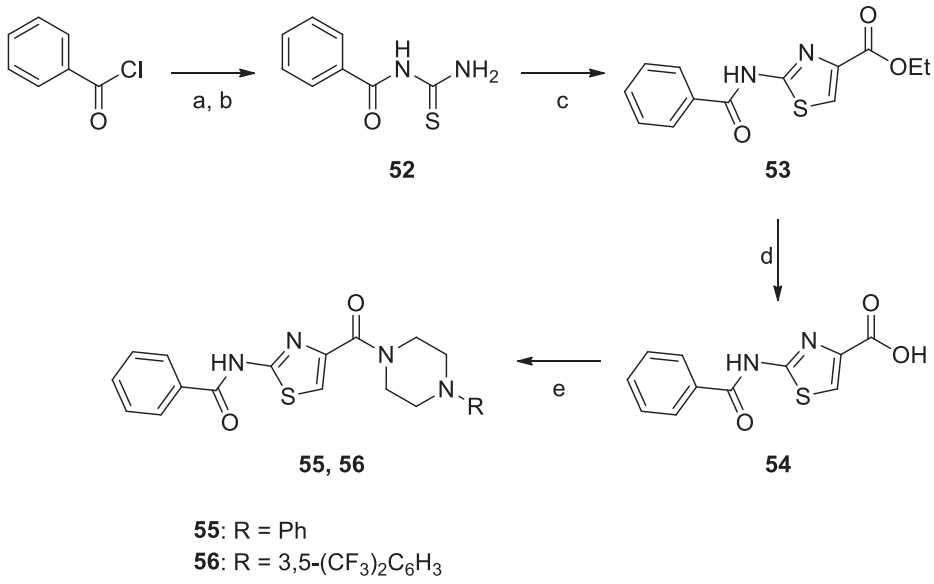


**Scheme 4.** Synthesis of thiazoles **55** and **56.** Reagents and conditions: (a) KSCN, acetone, 30 min, RT; (b) $NH_4OH$, 30 min, RT; (c) ethyl bromopyruvate, EtOH, 2 h, reflux; (d) NaOH, $H_2O$, EtOH, 4 h, 60 °C; (e) amine, EDC × HCl, HOBt, $CH_2Cl_2$, 14 h, 0 °C → RT.

repeating the inhibition experiments in the presence of Triton X-100 (0.01% (v/v)) [46]. All compounds investigated on mCEase showed a drop in inhibitory activity under these conditions, with thiazole **56** having been exemplarily characterized as promiscuous inhibitor by determination of the inhibitor concentration resulting in 50% inhibition ($IC_{50}$) in the absence and presence of detergent (Fig. S12). In contrast, promiscuous inhibition of FAAH by **56** ($IC_{50}$ = 52.4 μM, Fig. S13) could be excluded due to the applied assay conditions, [47] since the respective assay buffer already contained Triton X-100 (0.1% (w/v)) in the initial screening and the complete solubility of **56** at the chosen concentrations had been shown by UV–Vis spectroscopy (Fig. S8) according to Huang et al. [48].

In case of hMAGL, compounds **21** and **42** (analyzed at a single concentration of 25 μM) showed a detergent-sensitive behavior, whereas inhibition by quinazolinones **85**, **96** and **97** was not much influenced by Triton X-100 (Fig. 2, Figs. S14A and S14B). The latter three inhibitors exhibited values of $IC_{50}$ between 19.6 μM and 41.4 μM, which were only slightly increased by factors of 1.2–1.8 when detergent was added. The comparable inhibitory behavior of **85**, **96** and **97** can be attributed to the structural similarities of the three compounds (Schemes 5 and 6), which only differ in the alkyl chain spacer between the quinazolinone and the urea motifs, containing three, four and five methylene groups, respectively. The insensitivity of the MAGL inhibition towards the presence of Triton X-100, which had been observed for compounds **85**, **96** and **97**, might be explained by the inhibitor concentrations chosen for the $IC_{50}$ determinations. At these concentrations,

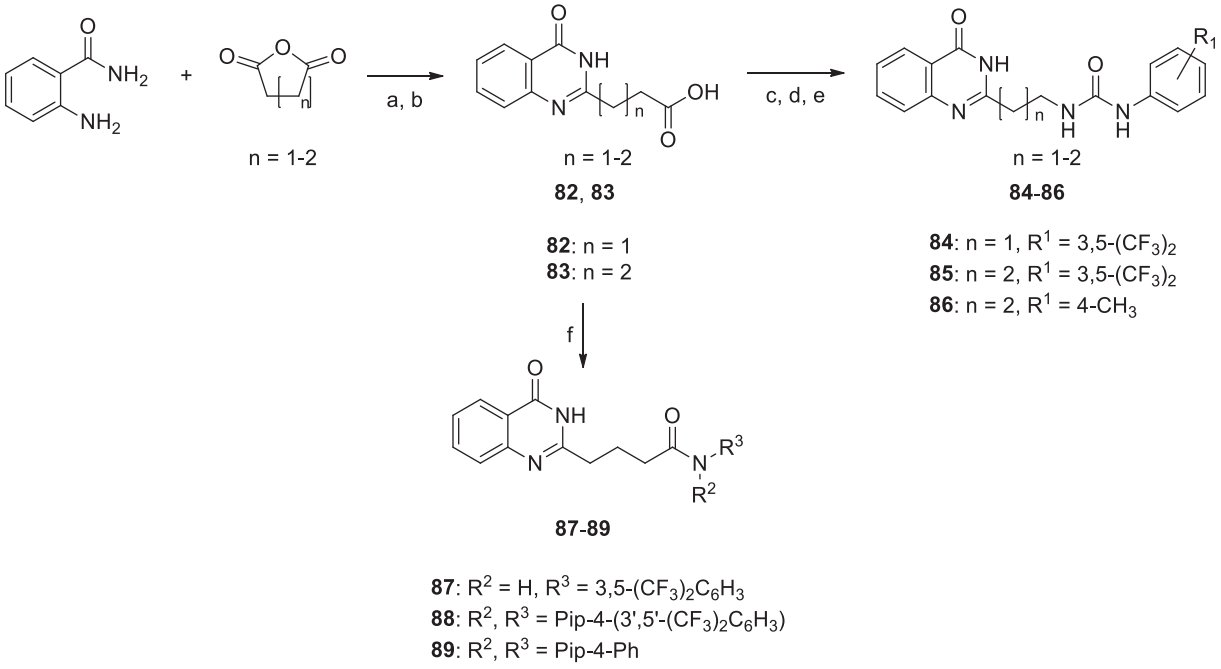


**Scheme 5.** Synthesis of quinazolinones **84–89**. Reagents and conditions: (a) benzene/diethyl ether/1,4-dioxane (2:2:1), 2 h, RT; (b) NaOH, EtOH, 40 min, 0 °C → RT; (c) diphenylphosporyl azide, TEA, acetone, 3 h, RT; (d) xylene, 20 min, 135 °C; (e) aniline, 14 h, reflux; (f) amine, EDC × HCl, HOBt, DMF, 14 h, 0 °C → RT. Pip, 1,4-disubstituted piperazine.

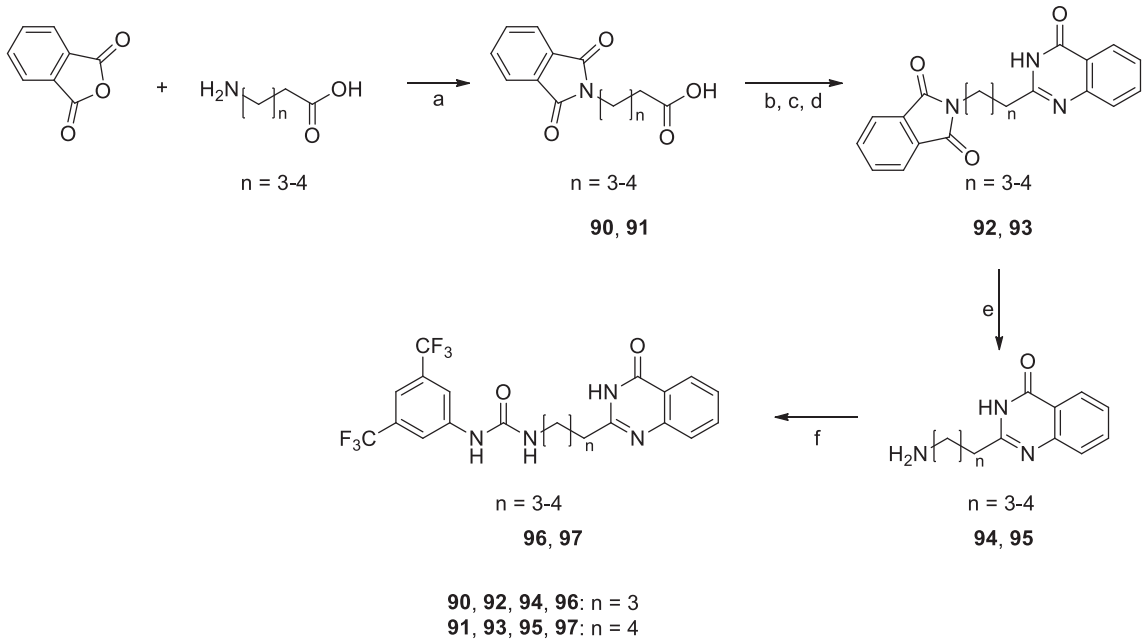


**Scheme 6.** Synthesis of quinazolinones **96** and **97**. Reagents and conditions: (a) neat, 3 h, 170 °C; (b) $SOCl_2$, toluene, 14 h, 0 °C → RT; (c) anthranilamide, TEA, THF, 5 h, 0 °C → RT; (d) diphenyl ether, 1 h, 220 °C; (e) hydrazine hydrate, MeOH, 4 h, reflux; (f) 3,5-bis(trifluoromethyl)phenyl isocyanate, $CHCl_3$, 14 h, RT.

**Table 1**
Residual enzymatic activities of hMAGL, hFAAH and mCEase in the presence of selected compounds.

| | Residual enzymatic activity (%) at [I] = 25 μM[a] | | |
|---|---|---|---|
| Compd | hMAGL | hFAAH | mCEase |
| **21** | *59.8 ± 1.9*[b] | 65.7 ± 6.1 | 102 ± 3 |
| **32** | 83.8 ± 2.5 | 89.0 ± 1.3 | *44.2 ± 0.8*[b] |
| **34** | 94.6 ± 1.9 | 88.7 ± 2.8 | *55.5 ± 0.7*[b] |
| **42** | *59.6 ± 3.4*[b] | 80.0 ± 2.4 | 66.5 ± 3.3 |
| **56** | 88.6 ± 3.5 | **48.0 ± 8.7**[c] | *29.8 ± 1.0*[d] |
| **85** | **56.4 ± 2.6**[d] | 93.4 ± 2.2 | *55.8 ± 2.6*[b] |
| **96** | **64.5 ± 9.1**[d] | 82.1 ± 2.0 | *63.7 ± 2.4*[b] |
| **97** | **58.1 ± 3.7**[d] | 88.4 ± 2.5 | 71.2 ± 2.4 |
| **106**[e] | 64.1 ± 10.4 | 78.2 ± 3.8 | **5.25 ± 1.63** |
| **107**[e] | 68.5 ± 5.3 | 85.0 ± 2.0 | **15.6 ± 3.1** |

[a] Mean ± SEM value (n = 3–4). Residual activity ≤ 65% results in $IC_{50}$ ≤ 46 μM. Values in *italics* and **bold** represent enzyme-inhibitor interactions proven to be promiscuous and shown to be not affected by promiscuous inhibition, respectively.

[b] Residual activities in the presence of Triton X-100 (0.01% (v/v)): **21** and **42** on hMAGL: 82.8 ± 2.3%, and 87.7 ± 3.9%, respectively; **32**, **34**, **85** and **96** on mCEase, 73.6 ± 1.4%, 101 ± 5%, 95.1 ± 1.0% and 93.1 ± 2.3% respectively.

[c] Determination of $IC_{50}$ on hFAAH in the presence of Triton X-100 (0.1% (w/v)) was done as shown in Fig. S13.

[d] Determination of $IC_{50}$ and checking for promiscuous inhibition with Triton X-100 (0.01% (v/v)) were done as shown in Fig. S14A (**85** on hMAGL), Fig. 2 (**96** on hMAGL), Fig. S14B (**97** on hMAGL) and Fig. S12 (**56** on mCEase).

[e] ω-Phthalimidoalkyl 3,5-bis(trifluoromethyl)phenyl ureas investigated in a previous study [43].

the compounds were shown to be completely soluble under MAGL assay conditions by means of UV/Vis spectroscopy (Figs. S9–S11) [48].

### 2.3. Determination of $K_i$ and mode of inhibition of quinazolinone 96 on MAGL

To obtain further insights into the inhibition of hMAGL by compounds of the class of quinazolinones, we first analyzed the reversibility of the enzyme-inhibitor interaction in case of **96**. For this purpose, we determined the dependency of $IC_{50}$ on the pre-incubation time of inhibitor and enzyme before starting the enzymatic reaction. As previously shown [43,49], irreversibly acting compounds, such as the potent MAGL inhibitor JZL 184 (**108**, Figs. 1 and 2) [50], show a strong increase in inhibitory potency after pre-incubation with hMAGL ($IC_{50}$ = 0.013 μM after 30 min pre-incuabation [43]). In contrast, values of $IC_{50}$ for the inhibition of hMAGL by **96** showed no time-dependency within 60 min (Fig. 3), which strongly points to a reversible mode of interaction. Similar results have been obtained with other reversible inhibitors of hMAGL [51], including compounds **6** [32], **8** [34], **9** [35], and **11** [37] (Fig. 1).

Binding of **96** to hMAGL was quantified by determining the dissociation constant, $K_i$, and the mode of inhibition. Enzymatic rates obtained with various concentrations of the substrate 4-NPB and inhibitor **96** were analyzed by nonlinear regression (Michaelis-Menten plot, Fig. 4) using an equation of mixed-type inhibition [52]. This determination yielded values of $K_i$ = 15.4 μM and α = 8.94, with the latter parameter indicating a mixed-type inhibition with a pronounced competitive component. The mode of inhibition was confirmed by subjecting the original data to several linear transformation methods as shown in Fig. S15. Literature-known MAGL inhibitors, such as compounds **4** [30] and **5** [31] (Fig. 1) have been shown to act in a non-competitive manner, whereas **6–9** [32–35] exhibit an extraordinarily clear competitive behavior with parameter α > 10000.

The ω-quinazolinonylalkyl aryl urea **96** represents a novel chemical entity that acts as a reversible inhibitor of the serine hydrolase hMAGL. So far, there is no quinazolinone known to affect the activity of MAGL. In contrast, the urea motif is quite common in potent irreversible MAGL inhibitors [23–25]. Those ureas which most probably act in a reversible manner often show lower inhibitory activities [53,54] or behave as activator of MAGL [55]. Recently, we have discovered that ω-phthalimidoalkyl 3,5-bis(trifluoromethyl)phenyl ureas **106** and **107** (Fig. 1, Table 1), which are structurally related to quinazolinones **85** and **96**, respectively, exhibit inhibitory potencies on hMAGL and hFAAH comparable to those of the two quinazolinones. However, in contrast to **85** and **96**, their phthalimide analogs affected both mCEase and the respective human isoenzyme (hCEase) to greater extent (Table 1) [43]. In addition to **96**, only few chemical entities have been identified so far that inhibit MAGL in a reversible manner. Examples for

A)

| Compd | $IC_{50}$ (μM) | |
|---|---|---|
| Triton X-100 | none | 0.01% (v/v) |
| JZL 184 | 0.314 ± 0.005[a] | n.d.[b] |
| **85** | 41.4 ± 7.8 | 53.9 ± 7.4[a] |
| **96** | 19.6 ± 3.5 | 23.4 ± 2.4 |
| **97** | 23.9 ± 3.0 | 42.7 ± 6.5 |

[a] Mean ± SEM value, $n = 4$, [b] n.d., not determined.

B)

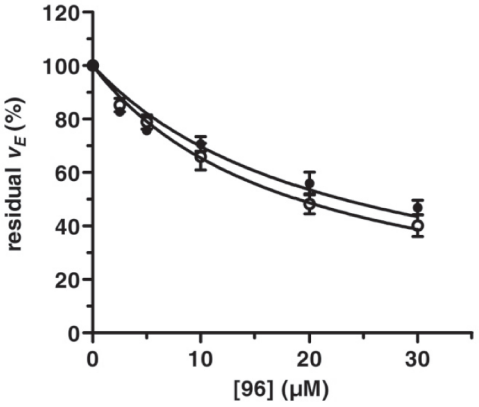


**Fig. 2.** (A) Values of $IC_{50}$ for the inhibition of hMAGL by reference compound JZL 184 (**1 0 8**) (taken from [43]) and the quinazolinones **85**, **96** and **97**, which were determined without pre-incubation of enzyme and inhibitor. (B) Exemplarily shown are residual enzymatic activities (mean ± SEM values of three independent triplicate experiments) in the presence of **96** relative to the control in the absence of compound **96** ($v_E$ = 100%) without (open circles) and with (full circles) Triton X-100 (0.01% (v/v)). $IC_{50}$ (mean ± SEM value, $n = 3$) of **85**, **96** and **97** were determined according to the equation $v_E = 100\%/(1 + ([I]/IC_{50}))$, with $v_E$ representing the rate of enzymatic product formation in the presence of inhibitor, I. $IC_{50}$ values of **85**, **96** and **97** obtained in the absence and presence of Triton X-100 were not significantly different from each other ($P > 0.05$, unpaired Student's $t$ test).

such compounds are summarized in Fig. 1, with the first generation inhibitor **7** [33] (competitive) and the second generation inhibitor **4** [30] (non-competitive) exhibiting $K_i$ values in a similar range to that of **96**.

### 2.4. Molecular docking

To identify new reversible inhibitors of MAGL, we initially performed a virtual screening of compounds originated from the ZINC database and structures derived thereof using the docking program Glide (version 6.1, Schrödinger, LLC, New York, NY, 2013). As a target for the docking experiments, we chose the crystal structure of hMAGL co-crystallized with the non-covalent binding inhibitor ZYH (**3**, Fig. 1). Validation of the docking procedure was done by removing the co-crystallized ZYH and re-docking of the structure resulting in an excellent reproduction of the inhibitor orientation (rmsd of 0.6 Å). The initial docking was performed in the standard precision mode of glide and afterwards, a selection of the best matching compounds was re-docked in the extra precise mode. The resulting library is depicted in Table S1. Our initial docking results indicated that representatives of various structural classes might be able to interact with the active site of hMAGL in a productive manner. Hence all compounds of Table S1 were synthesized and analyzed for their potential to decrease the activity of hMAGL. The quinazolinone **96** possessing suitable ADME properties (Table S1) was identified as most promising candidate for further investigation.

To have an idea of a possible interaction of **96** with hMAGL, the computed positioning of this predominantly competitive acting compound in the enzyme's active site (Figs. 5 and S16) was analyzed in comparison to the orientation of the re-docked ZYH (**3**) (Fig. S16). Whereas the quinazolinone moiety of **96** interacts via π-stacking with Tyr194 similar to ZYH's pyrimidine ring, the bulky 3,5-bis(trifluoromethyl)phenyl substituent of **96** "projects into a more spacious void"[29] that is occupied by the hydrophobic cyclohexane portion of ZYH. The urea motif in **96** confers planarity to the portion of the inhibitor adjacent to the terminal bulky moiety as found for the benzoxazole ring within ZYH. A comparison of the structure of co-crystallized ZYH with that of the docked substrate 2-arachidonyl glycerol revealed that the cyclohexane and benzoxazole portions of the inhibitor occupy the same space as the arachidonyl moiety of the natural substrate (Figs. 4B and 4C in Schalk-Hihi et al. [29]). The increased inhibitory activity of ZYH ($IC_{50}$ = 10 nM)[28] in comparison to **96** might be explained by the two hydrogen bonds formed between the carbonyl oxygen atom of ZYH and the backbone NH groups of Ala51 and Met123 (oxyanion hole of hMAGL) which are absent in the docking structure of

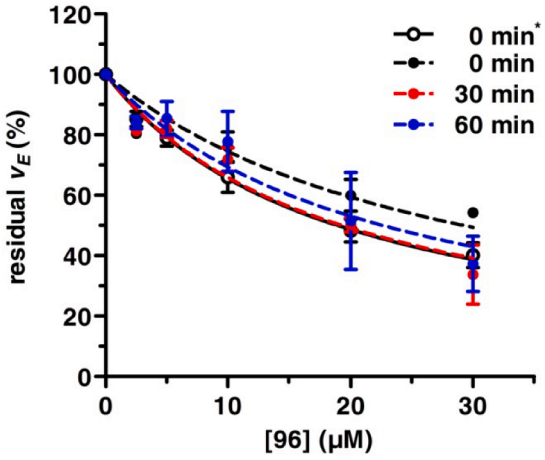


| Incubation time | $IC_{50}$ (μM) |
|---|---|
| 0 min* | 19.6 ± 3.5 |
| 0 min | 29.7 ± 3.6 |
| 30 min | 19.5 ± 1.4 |
| 60 min | 20.2 ± 3.4 |

**Fig. 3.** Reversible inhibition of hMAGL by **96**. Values of $IC_{50}$ for the inhibition of hMAGL by quinazolinone **96** were determined after pre-incubation of enzyme and inhibitor for 0, 30, and 60 min. Shown are residual enzymatic activities (mean ± SEM values of three independent triplicate experiments) relative to the control without inhibitor ($v_E$ = 100%). *Data of a previous $IC_{50}$ determination shown in Fig. 2 (performed in the absence of Triton X-100 without pre-incubation of MAGL with **96**) are depicted again for reasons of comparison. $IC_{50}$ (mean ± SEM value, $n = 3$) was calculated according to the equation $v_E = 100\%/(1 + ([I]/IC_{50}))$. Values of $IC_{50}$ obtained without pre-incubation within a previous analysis (see also Fig. 2) and this series of experiments were not significantly different from each other ($P > 0.05$, unpaired Student's $t$ test). Furthermore, a one-way analysis of variance (ANOVA) with Tukey's multiple comparison test of the experiments of this series without pre-incubation and both with 30 min and 60 min pre-incubation yielded no significant differences ($P > 0.05$) between the respective values of $IC_{50}$.

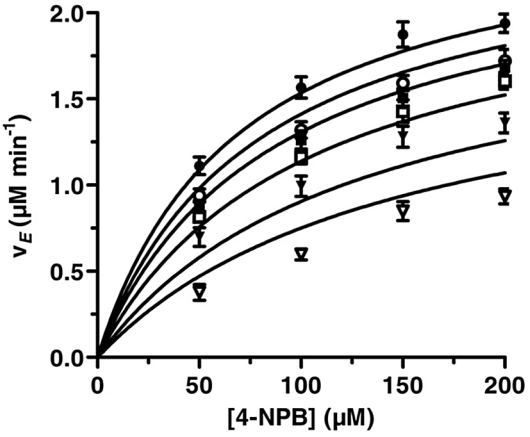


**Fig. 4.** Determination of the dissociation constant, $K_i$, and the mode of inhibition for the interaction of hMAGL (20 ng mL$^{-1}$) with compounds **96**. Depicted is a Michaelis-Menten plot with enzymatic rates from four independent triplicate experiments (mean ± SEM values). Concentrations of **96** were as follows: 0 µM (●), 2.5 µM (○), 5 µM (■), 10 µM (□), 20 µM (▼), and 30 µM (▽). Nonlinear regression analysis was performed using an equation of mixed-type inhibition [52] in dependence on the concentration of both the substrate 4-NPB and inhibitor **96**, resulting in values $K_i$ = 15.4 ± 1.8 µM and α = 8.94 ± 5.04 (mean ± SEM values, $n$ = 4).

**96**. Although interaction of quinazolinone **96** with hMAGL lacks hydrogen bonds and is predominantly mediated by both π-π and lipophilic interactions, we observed a strong similarity to the binding mode of ZYH (Fig. S16).

## 3. Conclusions

In the search of reversible inhibitors of MAGL we have initially chosen an *in silico* approach to explore a variety of compound classes for their ability to effectively bind to hMAGL. Synthesis of primary hits and their biochemical investigation on hMAGL as well as on the related enzymes hFAAH and mCEase by spectrophotometric and fluorometric assays led to the identification of ω-quinazolinonylalkyl aryl ureas as a new class of inhibitors of the former enzyme which exhibit $IC_{50}$ values in the range of 20–41 µM. As exemplarily shown for **96**, i.e. the most potent derivative ($K_i$ = 15.4 µM) of the investigated ω-quinazolinonylalkyl aryl ureas, this class of compounds interacts with MAGL in a reversible manner, since no time-dependency of the inhibitory potency has been observed. Both a kinetic analysis and a molecular docking study with **96** indicated that this compound occupies the substrate binding pocket of MAGL and, thus, exhibits a mixed-type inhibition with a predominant competitive behavior (α = 8.94). The activities of hFAAH and mCEase were either inhibited to lesser extent or affected in a detergent-sensitive manner by the ω-quinazolinonylalkyl aryl ureas. In conclusion, our findings indicate that ω-quinazolinonylalkyl aryl ureas, in particular **96**, may be leads worth to be pursued to yield potent reversible MAGL inhibitors for studying the effects of inhibiting this enzyme in various diseases.

## 4. Experimental section

General information about material and methods can be found in the Supplement.

### 4.1. Chemistry

#### 4.1.1. General procedures A/B/C for the 1-ethyl-3-(3-dimethylaminopropyl) carbodiimide mediated amide coupling reactions

To a stirred solution of 1 eq amine, 1.2 eq (A) or 1 eq (B/C) carboxylic acid and 1.15 eq 1-hydroxybenzotriazole hydrate dissolved in DCM or DMF was added 1.25 eq 1-ethyl-3-(3-dimethylaminopropyl)carbodiimide hydrochloride at 0 °C in one portion. The reaction was warmed to room temperature and stirred for further 14 h. After completion of the reaction in DMF, the solvent was evaporated and the crude product was purified by flash chromatography or recrystallized if mentioned. When DCM was used as solvent, the mixture was washed three times with a saturated sodium carbonate solution (A/B/C) followed by 10% (w/w) hydrochloric acid (C), the organic layer was separated, the solvent was evaporated under reduced pressure and the crude product was purified by flash chromatography or recrystallized if mentioned.

#### 4.1.2. General procedure D for the Suzuki coupling

Under an argon atmosphere 1 eq bromoaniline, 1 eq 3,5-bis(trifluoromethyl)phenylboronic acid, 0.05 eq tri(*o*-tolyl)phosphine and 2 eq potassium carbonate were added to a solution containing 8 mL DMF, 4 mL toluene and 2 mL water. The mixture was degassed under reduced pressure and purged with argon for 30 min. Then, 0.0125 eq palladium(II) acetate was added and the mixture was heated to 80 °C for 1.5 h. The solvent was evaporated in vacuo and the crude product was purified by flash chromatography.

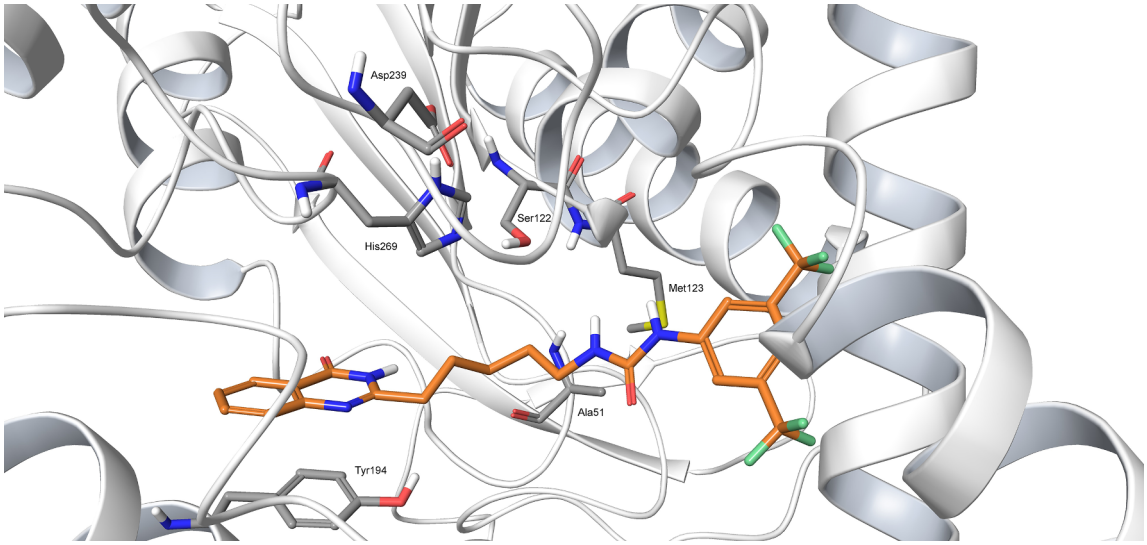


**Fig. 5.** Result of docking quinazolinone **96** (orange carbon atoms) into the active site of hMAGL (PDB: 3PE6). Non-polar hydrogen atoms are omitted. Residues of the catalytic triad (Ser122-His269-Asp239) and those of the oxyanion hole (Ala51, Met123) are shown.

*4.1.3. Synthetic procedures for selected compounds listed in Table 1*

*4.1.3.1. N-(3′,5′-Bis(trifluoromethyl)-[1,1′-biphenyl]-4-yl)-2-((3-phenylpropyl)sulfonyl)acetamide (**21**).* The reaction was performed according to the general procedure B with 0.24 g 2-((3-phenylpropyl) sulfonyl)acetic acid (**16**, 1.0 mmol), 0.31 g 3′,5′-bis(trifluoromethyl)-[1,1′-biphenyl]-4-amine (**104**, 1.0 mmol), 0.16 g HOBt (1.15 mmol) and 0.24 g EDC × HCl (1.25 mmol) in 15 mL DCM. The crude product was purified via column chromatography (35% EtOAc/*n*-hexane), yielding a white solid (0.27 g, 0.51 mmol, 51%); $R_f$ = 0.30 (35% EtOAc/*n*-hexane); mp: 211 °C; $^1$H NMR (300 MHz, DMSO-$d_6$) $\delta$ = 10.63 (s, 1H), 8.31 (s, 2H), 8.05 (s, 1H), 7.89 (d, $J$ = 8.5 Hz, 2H), 7.74 (d, $J$ = 8.6 Hz, 2H), 7.26 (m, 5H), 4.33 (s, 2H), 3.33 (m, 2H), 2.76 (t, $J$ = 7.6 Hz, 2H), 2.08 (m, 2H); $^{13}$C NMR (75 MHz, DMSO-$d_6$) $\delta$ = 160.77, 142.03, 140.60, 139.12, 132.33, 130.95 (q, $J$ = 32.8 Hz), 128.42, 128.37, 127.98, 126.86, 126.12, 123.36 (q, $J$ = 273.0 Hz), 120.52, 119.69, 59.28, 52.42, 33.44, 23.03; IR $\tilde{\nu}$ [cm$^{-1}$] = 3675 (m), 2987–2901 (s), 2360 (w), 2173 (w), 2119 (w), 1926 (w), 1707 (w), 1394 (m), 1250 (m), 1066 (s), 891 (m); HR-MS (ESI) *m/z* calcd for $C_{25}H_{21}F_6NO_3S$: 530.12191 $(M+H)^+$, found: 530.12209.

*4.1.3.2. 2-(4-(3,5-Bis(trifluoromethyl)phenyl)piperazin-1-yl)-2-oxo-N-phenylacetamide (**32**).* The reaction was performed according to the general procedure A with 0.40 g 2-oxo-2-(phenylamino)acetic acid (**27**, 2.4 mmol), 0.60 g 1-(3,5-bis(trifluoromethyl)phenyl)piperazine (**105**, 2.0 mmol), 0.31 g HOBt (2.3 mmol) and 0.48 g EDC × HCl (2.5 mmol) in 30 mL DCM. The crude product was purified via column chromatography (100% DCM), yielding a white solid (0.60 g, 1.35 mmol, 67%); $R_f$ = 0.29 (100% DCM); mp: 122 °C; $^1$H NMR (300 MHz, DMSO-$d_6$) $\delta$ = 10.80 (s, 1H), 7.67 (d, $J$ = 7.9 Hz, 2H), 7.52 (s, 2H), 7.36 (m, 3H), 7.13 (t, $J$ = 7.3 Hz, 1H), 3.69 (m, 4H), 3.48 (m, 4H); $^{13}$C NMR (75 MHz, DMSO-$d_6$) $\delta$ = 162.49, 161.61, 151.25, 137.78, 131.14 (q, $J$ = 32.3 Hz), 128.87, 124.33, 123.54 (q, $J$ = 272.9 Hz), 119.83, 114.68, 110.59, 47.38, 46.75, 45.04, 40.55; IR $\tilde{\nu}$ [cm$^{-1}$] = 3307 (w), 2363 (w), 1687 (m), 1633 (m), 1395 (m), 1280 (s), 1178 (m), 1128 (s), 963 (m), 761 (m), 696 (m); HR-MS (ESI) *m/z* calcd for $C_{20}H_{17}F_6N_3O_2$: 446.12977 $(M+H)^+$, found: 446.13016.

*4.1.3.3. N-(3,5-Bis(trifluoromethyl)phenyl)-2-(4-(3,5-bis(trifluoromethyl)phenyl)piperazin-1-yl)-2-oxoacetamide (**34**).* The reaction was performed according to the general procedure A with 0.72 g 2-((3,5-bis(trifluoromethyl)phenyl)amino)-2-oxoacetic acid (**28**, 2.4 mmol), 0.60 g 1-(3,5-bis(trifluoromethyl)phenyl)piperazine (**105**, 2.0 mmol), 0.31 g HOBt (2.3 mmol) and 0.48 g EDC × HCl (2.5 mmol) in 30 mL DCM. The crude product was purified via column chromatography (65% DCM/*n*-hexane), yielding a yellow solid (0.53 g, 0.91 mmol, 45%); $R_f$ = 0.25 (65% DCM/*n*-hexane); mp: 166 °C; $^1$H NMR (300 MHz, DMSO-$d_6$) $\delta$ = 8.71 (s, 1H), 7.86 (m, 4H), 7.36 (s, 4H), 6.23 (t, $J$ = 5.6 Hz, 1H), 3.61 (t, $J$ = 6.9 Hz, 2H), 3.11 (dd, $J$ = 12.6 Hz, 6.4 Hz, 2H), 1.75 (p, $J$ = 6.7 Hz, 2H); $^{13}$C NMR (75 MHz, DMSO-$d_6$) $\delta$ = 161.92, 161.36, 151.23, 139.76, 130.86 (q, $J$ = 32.8 Hz), 123.10 (q, $J$ = 272.4 Hz), 119.79, 117.26, 114.67, 110.61, 47.45, 46.75, 45.08, 40.94; IR $\tilde{\nu}$ [cm$^{-1}$] = 3671 (m), 3294 (w), 2987–2901 (s), 2357 (w), 1643 (m), 1394 (s), 1274 (s), 1066 (s), 893 (m), 683 (m); HR-MS (ESI) *m/z* calcd for $C_{22}H_{15}F_{12}N_3O_2$: 582.10454 $(M+H)^+$, found: 582.10470; elemental analysis calcd for $C_{22}H_{15}F_{12}N_3O_2$: C 45.45, H 2.60, N 7.23, found: C 45.45, H 2.64, N 7.26.

*4.1.3.4. 3-((3,5-Bis(trifluoromethyl)phenyl)amino)-4-((3-phenylpropyl)amino)cyclobut-3-ene-1,2-dione (**42**).* 3-Phenyl-1-propylamine (0.14 mL, 0.135 g, 1.0 mmol) were added to a solution of 0.353 g 3-((3,5-bis(trifluoromethyl)phenyl)amino)-4-ethoxycyclobut-3-ene-1,2-dione (**40**, 1.0 mmol) dissolved in 10 mL DCM at room temperature. After 24 h, a white precipitate was formed. The solid was filtered off and washed with ice-cold DCM. The product was obtained as a white solid (0.15 g, 0.38 mmol, 38%); mp: 202 °C; $^1$H NMR (300 MHz, DMSO-$d_6$) $\delta$ = 10.15 (s, 1H), 8.02 (s, 2H), 7.71 (d, $J$ = 27.2 Hz, 1H), 7.63 (s, 1H), 7.23 (m, 5H), 3.65 (d, $J$ = 4.7 Hz, 2H), 2.66 (t, $J$ = 7.6 Hz, 2H), 1.90 (m, 2H); $^{13}$C NMR (75 MHz, DMSO-$d_6$) $\delta$ = 180.45, 169.85, 162.37, 141.12, 131.31 (q, $J$ = 31.9 Hz), 128.33, 128.23, 125.85, 123.20 (q, $J$ = 273.1 Hz), 117.97, 114.62, 43.60, 32.19, 31.98; IR $\tilde{\nu}$ [cm$^{-1}$] = 3674 (m), 3221 (w), 2987–2901 (s), 2341 (w), 2186 (w), 2126 (w), 1929 (w), 1787 (w), 1657 (m), 1565 (m), 1380 (s), 1277 (m), 1132 (s), 1066 (s), 894 (m), 697 (m); HR-MS (ESI) *m/z* calcd for $C_{21}H_{16}F_6N_2O_2$: 443.11887 $(M+H)^+$, found: 443.11886; elemental analysis calcd for $C_{21}H_{16}F_6N_2O_2$: C 57.02, H 3.65, N 6.33, found: C 57.22, H 3.89, N 6.53.

*4.1.3.5. N-(4-(4-(3,5-Bis(trifluoromethyl)phenyl)piperazine-1-carbonyl)thiazol-2-yl)benzamide (**56**).* The reaction was performed according to the general procedure A with 0.60 g 2-benzamidothiazole-4-carboxylic acid (**54**, 2.4 mmol), 0.60 g 1-(3,5-bis(trifluoromethyl)phenyl) piperazine (**105**, 2.0 mmol), 0.31 g HOBt (2.3 mmol) and 0.48 g EDC × HCl (2.5 mmol) in 30 mL DMF. The crude product was purified via column chromatography (90% $CHCl_3$/acetone), yielding a yellow solid (0.72 g, 1.37 mmol, 68%); $R_f$ = 0.33 (90% $CHCl_3$/acetone); mp: 219 °C; $^1$H NMR (300 MHz, DMSO-$d_6$) $\delta$ = 12.80 (s, 1H), 8.12 (d, $J$ = 7.1 Hz, 2H), 7.71 (s, 1H), 7.65 (t, $J$ = 7.3 Hz, 1H), 7.56 (t, $J$ = 7.4 Hz, 2H), 7.51 (s, 2H), 7.33 (s, 1H), 3.86 (s, 4H), 3.46 (s, 4H); $^{13}$C NMR (75 MHz, DMSO-$d_6$) $\delta$ = 165.52, 162.85, 158.16, 151.43, 144.39, 132.70, 131.91, 131.15 (q, $J$ = 32.3 Hz), 128.59, 128.21, 123.58 (q, $J$ = 273.0 Hz), 117.80, 114.55, 110.42, 47.27; IR $\tilde{\nu}$ [cm$^{-1}$] = 3670 (w), 2988–2901 (s), 1360 (w), 1610 (m), 1537 (m), 1394 (m), 1273–1232 (m), 1066 (s), 865 (w), 698 (w); HR-MS (ESI) *m/z* calcd for $C_{23}H_{18}F_6N_4O_2S$: 529.11274 $(M+H)^+$, found: 529.11272.

*4.1.3.6. 1-(3,5-Bis(trifluoromethyl)phenyl)-3-(3-(4-oxo-3,4-dihydroquinazolin-2-yl)propyl)urea (**85**).* 4-(4-Oxo-3,4-dihydroquinazolin-2-yl)butanoic acid (0.70 g, 3 mmol), 1.0 mL triethylamine (**83**, 0.73 g, 7.2 mmol) and 0.78 mL diphenylphosphoryl azide (0.99 g, 3.6 mmol) in 100 mL acetone were stirred for 3 h at room temperature. The solvent was removed in vacuo, the resulting residue was dissolved in 40 mL xylene and heated to 135 °C for 20 min. 3,5-Bis(trifluoromethyl)aniline (0.56 mL, 0.83, 3.6 mmol) was added and the mixture was refluxed for further 14 h. Then, the reaction mixture was cooled to room temperature, the solvent was evaporated in vacuo, and the crude product was purified by flash chromatography (30% acetone/*n*-hexane), yielding a white solid (105 mg, 0.23 mmol, 8%); $R_f$ = 0.20 (30% acetone/*n*-hexane); mp: 235 °C; $^1$H NMR (300 MHz, DMSO-$d_6$) $\delta$ = 12.19 (s, 1H), 9.23 (s, 1H), 8.07 (m, 3H), 7.76 (t, $J$ = 6.9 Hz, 1H), 7.58 (d, $J$ = 8.0 Hz, 1H), 7.53 (s, 1H), 7.45 (t, $J$ = 7.5 Hz, 1H), 6.56 (t, $J$ = 5.6 Hz, 1H), 3.20 (dd, $J$ = 12.7 Hz, 6.6 Hz, 2H), 2.65 (t, $J$ = 7.5 Hz, 2H), 1.93 (m, 2H); $^{13}$C NMR (101 MHz, DMSO-$d_6$) $\delta$ = 161.65, 156.94, 154.75, 148.81, 142.55, 134.08, 130.49 (q, $J$ = 32.5 Hz), 126.68, 125.79, 125.56, 123.29 (q, $J$ = 272.7 Hz), 120.78, 117.19, 113.26, 38.65, 31.83, 27.02; IR $\tilde{\nu}$ [cm$^{-1}$] = 3674 (w), 3329 (w), 2988–2901 (m), 2357 (w), 1686 (m), 1652 (m), 1392 (m), 1285 (m), 1173 (m), 1126 (s), 1066 (s), 887 (m); HR-MS (ESI) *m/z* calcd for $C_{20}H_{16}F_6N_4O_2$: 459.12502 $(M+H)^+$, found: 459.12531.

*4.1.3.7. 1-(3,5-Bis(trifluoromethyl)phenyl)-3-(4-(4-oxo-3,4-dihydroquinazolin-2-yl)butyl)urea (**96**).* 3,5-Bis(trifluoromethyl)phenyl isocyanate (0.35 mL, 0.51 g, 2 mmol) was added to solution of 0.44 g 2-(4-aminobutyl)quinazolin-4(3*H*)-one (**94**, 2 mmol) in 20 mL $CHCl_3$ and stirred for 14 h at room temperature. The solvent was removed in vacuo and the resulting residue was purified via column chromatography (30% acetone/DCM), yielding a white solid (0.49 g, 1.03 mmol, 51%); $R_f$ = 0.29 (30% acetone/DCM); mp: 215 °C; $^1$H NMR (300 MHz, DMSO-$d_6$) $\delta$ = 12.19 (s, 1H), 9.21 (s, 1H), 8.08 (s, 3H), 7.75 (t, $J$ = 7.0 Hz, 1H), 7.58 (d, $J$ = 8.0 Hz, 1H), 7.51 (s, 1H), 7.44 (t, $J$ = 7.4 Hz, 1H), 6.53 (t, $J$ = 5.3 Hz, 1H), 3.15 (dd, $J$ = 12.4 Hz, 6.3 Hz, 2H), 2.63 (t, $J$ = 7.5 Hz, 2H), 1.75 (dd, $J$ = 14.8 Hz, 7.7 Hz, 2H), 1.53 (dd, $J$ = 14.2 Hz, 6.8 Hz, 2H); $^{13}$C NMR (75 MHz, DMSO-$d_6$) $\delta$ = 161.83, 157.35, 154.81, 148.95, 134.26, 130.58 (q, $J$ = 32.4 Hz),

126.80, 125.94, 125.70, 123.40 (q, $J$ = 272.9 Hz), 120.83, 117.21, 113.33, 38.95, 34.18, 29.11, 24.21; IR $\tilde{\nu}$ [$cm^{-1}$] = 3675 (m), 2987–2901 (s), 1653 (m), 1558 (w), 1385 (m), 1250 (m), 1066 (s), 892 (m), 771 (w); HR-MS (ESI) $m/z$ calcd for $C_{21}H_{18}F_6N_4O_2$: 473.14067 $(M+H)^+$, found: 473.14103.

*4.1.3.8. 1-(3,5-Bis(trifluoromethyl)phenyl)-3-(5-(4-oxo-3,4-dihydroquinazolin-2-yl)pentyl)urea (**97**).* 3,5-Bis(trifluoromethyl)phenyl isocyanate (0.35 mL, 0.51 g, 2 mmol) was added to solution of 0.46 g 2-(5-aminopentyl)quinazolin-4(3*H*)-one (**95**, 2 mmol) in 20 mL $CHCl_3$ and stirred for 14 h at room temperature. The solvent was removed in vacuo and the resulting residue was purified via column chromatography (30% acetone/DCM), yielding a white solid (0.53 g, 1.09 mmol, 55%); $R_f$ = 0.43 (30% acetone/DCM); mp: 207 °C; $^1$H NMR (300 MHz, DMSO-$d_6$) $\delta$ = 12.16 (s, 1H), 9.17 (s, 1H), 8.07 (m, 3H), 7.74 (t, $J$ = 7.1 Hz, 1H), 7.58 (d, $J$ = 8.1 Hz, 1H), 7.52 (s, 1H), 7.44 (t, $J$ = 7.4 Hz, 1H), 6.47 (t, $J$ = 5.4 Hz, 1H), 3.11 (dd, $J$ = 12.5 Hz, 6.4 Hz, 2H), 2.61 (t, $J$ = 7.5 Hz, 2H), 1.76 (dt, $J$ = 14.8 Hz, 7.4 Hz, 2H), 1.50 (m, 2H), 1.37 (dd, $J$ = 14.3 Hz, 7.5, 2H); $^{13}$C NMR (75 MHz, DMSO-$d_6$) $\delta$ = 161.85, 157.41, 154.79, 148.97, 142.69, 134.22, 130.58 (q, $J$ = 32.5 Hz), 126.80, 125.89, 125.68, 123.41 (q, $J$ = 272.7 Hz), 120.82, 117.17, 113.31, 39.09, 34.47, 29.34, 26.51, 25.91; IR $\tilde{\nu}$ [$cm^{-1}$] = 3675 (m), 2987–2901 (s), 2360 (w), 2176 (w), 2119 (w), 1932 (w), 1682 (w), 1650 (w), 1612 (w), 1394 (m), 1250 (m), 1066 (s), 894 (m); HR-MS (ESI) $m/z$ calcd for $C_{22}H_{20}F_6N_4O_2$: 487.15632 $(M+H)^+$, found: 487.15653.

### 4.2. Biological activity

#### 4.2.1. mCEase assay

Activity of murine CEase was investigated as recently described by Dato et al. [43]. Inhibition of mCEase (40 ng $mL^{-1}$) was determined with 25 μM of compound without pre-incubation by starting the reaction with 200 μM 4-MUB (2.7 × $K_m$). The $IC_{50}$ value of compound **56** was determined under the same conditions with six inhibitor concentrations (2.5–40 μM). Residual enzymatic activity was calculated as percentage value relative to controls without inhibitor after correction for non-enzymatic hydrolysis of 4-MUB. Analysis of compounds **32**, **34**, **56**, **85** and **96** for promiscuous inhibition was done under the same conditions as described above in the presence of Triton X-100 (0.01% (v/v)).

#### 4.2.2. hMAGL assay

Activity of human MAGL was investigated as recently reported by Dato et al. [43]. Inhibition of hMAGL (20 ng $mL^{-1}$) was determined with 25 μM of compound without pre-incubation by starting the reaction with 200 μM 4-NPB (1.1 × $K_m$). Residual enzymatic activity was calculated as percentage value relative to controls without inhibitor after correction for non-enzymatic substrate hydrolysis. Values of $IC_{50}$ for hMAGL inhibition by **85** (5–60 μM), **96** (2.5–30 μM) and **97** (2.5–40 μM), respectively, were analyzed in the presence of five to seven inhibitor concentrations. Promiscuous behavior of the compounds was investigated by repeating the experiments with Triton X-100 (0.01% (v/v)) being present in the reaction mixture. The reversible character of the interaction of hMAGL with **96** was analyzed by determining the values of $IC_{50}$ without pre-incubation of enzyme and inhibitor and after 30 min and 60 min pre-incubation at 30 °C. Calculation of percentage enzymatic activities was done as described above. The dissociation constant $K_i$ and the mode of inhibition of compound **96** were determined with four different concentrations of 4-NPB (50–200 μM) and six different inhibitor concentrations (0–30 μM). Rates from experiments with hMAGL were corrected by the mean value of the corresponding rate obtained in the absence of enzyme and subjected to non-linear regression (equation of linear mixed-type inhibition) [52].

#### 4.2.3. FAAH assay

Activity of FAAH was investigated as recently reported by Dato et al. [45]. Screening for inhibition of FAAH (1 μg $mL^{-1}$) was performed with 10 μM D-MAP (1.2 × $K_m$) and 25 μM of compound to be analyzed without pre-incubation. $IC_{50}$ of **56** was determined under the same conditions but with seven inhibitor concentrations (2.5–50 μM). The enzymatic reaction was started with D-MAP. Residual enzymatic activity was calculated as percentage value relative to controls without inhibitor after correction for non-enzymatic hydrolysis of D-MAP.

### 4.3. Solubility of selected compounds

The solubility of the compounds **56**, **85**, **96** and **97** was investigated in 96-well microtiter plates (transparent BRANDplates® with F-bottom) in a volume of 200 μL at four to nine compound concentrations (**56**, **85** and **97**: 25–100 μM; **96**: 2.5–100 μM). For each experiment, 20 μL of compound solution (ten-fold concentrated) prepared in assay buffer with 25% (v/v) DMSO was added to 170 μL assay buffer (**56**: FAAH assay buffer; **85**, **96** and **97**: MAGL assay buffer), 5 μL DMSO and 5 μL enzyme buffer (**56**: FAAH enzyme buffer; **85**, **96**, **97**: MAGL enzyme buffer). UV/Vis spectra were measured in the range of 300–650 nm.

### 4.4. Molecular docking

Docking studies on hMAGL were performed using the Schrödinger Suite 2013–3 (Schrödinger, LLC, New York, NY, 2013), including the programs Glide (v.6.1) [56–58], LigPrep (v.2.8), Maestro (v.9.6) and the Protein Preparation Wizard containing the programs Epik (v.2.6) [59,60], Impact (v.6.1) and Prime (v.3.4). ADME property analysis, including parameters of Lipinski's rule of five (molecular weight, number of hydrogen bond donors, number of hydrogen bond acceptors, and predicted octanol-water partition coefficient) was done using QikProp (v.3.4) of the Schrödinger Suite. hMAGL crystal structure in complex with the co-crystallized non-covalent Inhibitor ZYH (**3**, PDB: 3PE6) was taken from the Protein Data Bank and pre-processed applying the Protein Preparation Wizard optimizing the hydrogen bonding network, pre-defining a pH value of 7.4 and removing possible crystallographic artifacts. Before the docking process, ligands were prepared with LigPrep adjusting a pH value of 7.4. For virtual screening, the unconstrained glide docking protocol was used, the grid box was centered on the co-crystallized inhibitor ZYH (**3**) and the initial docking simulation was performed using the default SP settings. Based on these results, promising candidates were re-docked with the standard XP settings, with additional settings "rewarding intramolecular hydrogen bonds" and "enhancing the planarity of conjugated pi-groups" being activated.

## Declaration of Competing Interest

The authors declare that they have no conflict of interests.

## Acknowledgements

The authors thank A. W. Schüller and R. Z. Uhl for assistance in screening for inhibitors of the three serine hydrolases. F. M. Dato and B. Goldfuss are grateful to the Fonds der Chemischen Industrie, the Deutsche Forschungsgemeinschaft (DFG GO-930-13), Bayer AG, BASF AG, Wacker Chemie AG, Evonik Industries AG, Raschig GmbH, Symrise AG, Solvay GmbH, and INEOS Manufacturing Deutschland GmbH for support as well as to the RRZK and the Department of Chemistry (University of Cologne) for the deployment of computer hardware (CHEOPS) and software. M. Pietsch thanks the Graduate Program in Pharmacology and Experimental Therapeutics of the University of Cologne and the Bayer Health Care AG.

## Appendix A. Supplementary material

Supplementary data to this article can be found online at https://doi.org/10.1016/j.bioorg.2019.103352.

## References


[1] M. Karlsson, J.A. Contreras, U. Hellman, H. Tornqvist, C. Holm, J. Biol. Chem. 272 (1997) 27218–27223.
[2] T.P. Dinh, D. Carpenter, F.M. Leslie, T.F. Freund, I. Katona, S.L. Sensi, S. Kathuria, D. Piomelli, Proc. Natl. Acad. Sci. USA. 99 (2002) 10819–10824.
[3] M. Duncan, A.D. Thomas, N.L. Cluny, A. Patel, K.D. Patel, B. Lutz, D. Piomelli, S.P.H. Alexander, K.A. Sharkey, Am. J. Physiol. Gastrointest. Liver Physiol. 295 (2008) G1255–G1265.
[4] D.K. Nomura, D.P. Lombardi, J.W. Chang, S. Niessen, A.M. Ward, J.Z. Long, H.H. Hoover, B.F. Cravatt, Chem. Biol. 18 (2011) 846–856.
[5] D.K. Nomura, J.Z. Long, S. Niessen, H.S. Hoover, S.-W. Ng, B.F. Cravatt, Cell 140 (2010) 49–61.
[6] H. Qin, Z.-H. Ruan, Cell Biochem. Biophys. 70 (2014) 33–36.
[7] R. Schwarz, R. Ramer, B. Hinz, Drug Metab. Rev. 50 (2018) 26–53.
[8] D.K. Nomura, B.E. Morrison, J.L. Blankman, J.Z. Long, S.G. Kinsey, M.C.G. Marcondes, A.M. Ward, Y.K. Hahn, A.H. Lichtman, B. Conti, B.F. Cravatt, Science 334 (2011) 809–813.
[9] R. Chen, J. Zhang, Y. Wu, D. Wang, G. Feng, Y.-P. Tang, Z. Teng, C. Chen, Cell Rep. 2 (2012) 1329–1339.
[10] J.R. Piro, D.I. Benjamin, J.M. Duerr, Y. Pi, C. Gonzales, K.M. Wood, J.W. Schwartz, D.K. Nomura, T.A. Samad, Cell Rep. 1 (2012) 617–623.
[11] N. Vujic, S. Schlager, T.O. Eichmann, C.T. Madreiter-Sokolowski, M. Goeritzer, S. Rainer, S. Schauer, A. Rosenberger, A. Woelfler, P. Doddapattar, R. Zimmermann, G. Hoefler, A. Lass, W.F. Graier, B. Radovic, D. Kratky, Atherosclerosis 244 (2016) 9–21.
[12] M.M. Mulvihill, D.K. Nomura, Life Sci. 92 (2013) 492–497.
[13] R.A. Kohnz, D.K. Nomura, Chem. Soc. Rev. 43 (2014) 6859–6869.
[14] G.F. Grabner, R. Zimmermann, R. Schicho, U. Taschler, Pharmacol. Ther. 175 (2017) 35–46.
[15] A.D. Quiroga, R. Lehner, Biochem. Pharmacol. 155 (2018) 233–241.
[16] M. Alhouayek, G.G. Muccioli, Trends Mol. Med. 18 (2012) 615–625.
[17] M. Alhouayek, J. Masquelier, G.G. Muccioli, Drug Discov. Today 19 (2014) 295–304.
[18] J. Zhang, Z. Liu, Z. Lian, R. Liao, Y. Chen, Y. Qin, J. Wang, Q. Jiang, X. Wang, J. Gong, Sci. Rep. 6 (2016) 35784.
[19] L. Ye, B. Zhang, E.G. Seviour, K.-X. Tao, X.-H. Liu, Y. Ling, J.-Y. Chen, G.-B. Wang, Cancer Lett. 307 (2011) 6–17.
[20] J.Z. Long, B.F. Cravatt, Chem. Rev. 111 (2011) 6022–6063.
[21] D.K. Nomura, J.E. Casida, Chem. Biol. Interact. 259 (2016) 211–222.
[22] J.E. Schlosburg, J.L. Blankman, J.Z. Long, D.K. Nomura, B. Pan, S.G. Kinsey, P.T. Nguyen, D. Ramesh, L. Booker, J.J. Burston, E.A. Thomas, D.E. Selley, L.J. Sim-Selley, Q.-S. Liu, A.H. Lichtman, B.F. Cravatt, Nat. Neurosci. 13 (2010) 1113–1119.
[23] C. Granchi, I. Caligiuri, F. Minutolo, F. Rizzolio, T. Tuccinardi, Expert Opin. Ther. Pat. 27 (2017) 1341–1351.
[24] A. Gil-Ordóñez, M. Martín-Fontecha, S. Ortega-Gutiérrez, M.L. López-Rodríguez, Biochem. Pharmacol. 157 (2018) 18–32.
[25] M. Feledziak, D.M. Lambert, J. Marchand-Brynaert, G.G. Muccioli, Recent Pat. CNS, Drug Discovery 7 (2012) 49–70.
[26] W. Tuo, N. Leleu-Chavain, J. Spencer, S. Sansook, R. Millet, P. Chavatte, J. Med. Chem. 60 (2017) 4–46.
[27] A.R. King, E.Y. Dotsey, A. Lodola, K.M. Jung, A. Ghomian, Y. Qiu, J. Fu, M. Mor, D. Piomelli, Chem. Biol. 16 (2009) 1045–1052.
[28] K. M. Chevalier, S. L. Dax, C. M. Flores, L. Liu, M. J. Macielag, M. E. McDonnell, M. I. Nelen, S. Prouty, M. Todd, S.-P. Zhang, B. Zhu, E. L. Nulton and J. Clemente, WO2010124121, 2010.
[29] C. Schalk-Hihi, C. Schubert, R. Alexander, S. Bayoumy, J.C. Clemente, I. Deckman, R.L. DesJarlais, K.C. Dzordzorme, C.M. Flores, B. Grasberger, J.K. Kranz, F. Lewandowski, L. Liu, H. Ma, D. Maguire, M.J. Macielag, M.E. McDonnell, T. Mezzasalma Haarlander, R. Miller, C. Milligan, C. Reynolds, L.C. Kuo, Protein Sci. 20 (2011) 670–683.
[30] J.A. Cisneros, E. Björklund, I. González-Gil, Y. Hu, Á. Canales, F.J. Medrano, A. Romero, S. Ortega-Gutiérrez, C.J. Fowler, M.L. López-Rodríguez, J. Med. Chem. 55 (2012) 824–836.
[31] G. Hernández-Torres, M. Cipriano, E. Hedén, E. Björklund, Á. Canales, D. Zian, A. Feliú, M. Mecha, C. Guaza, C.J. Fowler, S. Ortega-Gutiérrez, M.L. López-Rodríguez, Angew. Chem. Int. Ed. Engl. 53 (2014) 13765–13770.
[32] M. Aghazadeh Tabrizi, P.G. Baraldi, S. Baraldi, E. Ruggiero, L. De Stefano, F. Rizzolio, L. Di Cesare Mannelli, C. Ghelardini, A. Chicca, M. Lapillo, J. Gertsch, C. Manera, M. Macchia, A. Martinelli, C. Granchi, F. Minutolo, T. Tuccinardi, J. Med. Chem. 61 (2018) 1340–1354.
[33] T. Tuccinardi, C. Granchi, F. Rizzolio, I. Caligiuri, V. Battistello, G. Toffoli, F. Minutolo, M. Macchia, A. Martinelli, Bioorg. Med. Chem. 22 (2014) 3285–3291.
[34] C. Granchi, F. Rizzolio, S. Palazzolo, S. Carmignani, M. Macchia, G. Saccomanni, C. Manera, A. Martinelli, F. Minutolo, T. Tuccinardi, J. Med. Chem. 59 (2016) 10299–10314.
[35] C. Granchi, M. Lapillo, S. Glasmacher, G. Bononi, C. Licari, G. Poli, M. el Boustani, I. Caligiuri, F. Rizzolio, J. Gertsch, M. Macchia, F. Minutolo, T. Tuccinardi, A. Chicca, J. Med. Chem. 62 (2019) 1932–1958.
[36] C. Granchi, F. Rizzolio, V. Bordoni, I. Caligiuri, C. Manera, M. Macchia, F. Minutolo, A. Martinelli, A. Giordano, T. Tuccinardi, J. Enzyme Inhib. Med. Chem. 31 (2016) 137–146.
[37] C. Granchi, I. Caligiuri, E. Bertelli, G. Poli, F. Rizzolio, M. Macchia, A. Martinelli, F. Minutolo, T. Tuccinardi, J. Enzyme Inhib. Med. Chem. 32 (2017) 1240–1252.
[38] G. Bononi, C. Granchi, M. Lapillo, M. Giannotti, D. Nieri, S. Fortunato, M.E. Boustani, I. Caligiuri, G. Poli, K.E. Carlson, S.H. Kim, M. Macchia, A. Martinelli, F. Rizzolio, A. Chicca, J.A. Katzenellenbogen, F. Minutolo, T. Tuccinardi, Eur. J. Med. Chem. 157 (2018) 817–836.
[39] J. Aida, M. Fushimi, T. Kusumoto, H. Sugiyama, N. Arimura, S. Ikeda, M. Sasaki, S. Sogabe, K. Aoyama, T. Koike, J. Med. Chem. 61 (2018) 9205–9217.
[40] J.Z. Patel, S. Ahenkorah, M. Vaara, M. Staszewski, Y. Adams, T. Laitinen, D. Navia-Paldanius, T. Parkkari, J.R. Savinainen, K. Walczyński, J.T. Laitinen, T.J. Nevalainen, Bioorg. Med. Chem. Lett. 25 (2015) 1436–1442.
[41] J.J. Irwin, B.K. Shoichet, J. Chem. Inf. Model. 45 (2005) 177–182.
[42] J.J. Irwin, T. Sterling, M.M. Mysinger, E.S. Bolstad, R.G. Coleman, J. Chem. Inf. Model. 52 (2012) 1757–1768.
[43] F.M. Dato, M. Sheikh, R.Z. Uhl, A.W. Schüller, M. Steinkrüger, P. Koch, J.-M. Neudörfl, M. Gütschow, B. Goldfuss, M. Pietsch, ChemMedChem 13 (2018) 1833–1847.
[44] F.F. Wolf, H. Klare, B. Goldfuss, J. Org. Chem. 81 (2016) 1762–1768.
[45] F.M. Dato, A. Maaßen, B. Goldfuss, M. Pietsch, Anal. Biochem. 546 (2018) 50–57.
[46] B.Y. Feng, B.K. Shoichet, Nat. Protoc. 1 (2006) 550–553.
[47] L. Pohjala, P. Tammela, Molecules 17 (2012) 10774–10790.
[48] H. Huang, K. Nishi, H.-J. Tsai, B.D. Hammock, Anal. Biochem. 363 (2007) 12–21.
[49] E. Björklund, E. Norén, J. Nilsson, C.J. Fowler, Br. J. Pharmacol. 161 (2010) 1512–1526.
[50] J.Z. Long, W. Li, L. Booker, J.J. Burston, S.G. Kinsey, J.E. Schlosburg, F.J. Pavón, A.M. Serrano, D.E. Selley, L.H. Parsons, A.H. Lichtman, B.F. Cravatt, Nat. Chem. Biol. 5 (2009) 37–44.
[51] G. Poli, M. Lapillo, V. Jha, N. Mouawad, I. Caligiuri, M. Macchia, F. Minutolo, F. Rizzolio, T. Tuccinardi, C. Granchi, J. Enzyme Inhib. Med. Chem. 34 (2019) 589–596.
[52] I.H. Segel, Enzyme kinetics: Behavior and analysis of rapid equilibrium and steady-state enzyme systems, John Wiley & Sons, Hoboken, 1993.
[53] N. Ghafouri, G. Tiger, R.K. Razdan, A. Mahadevan, R.G. Pertwee, B.R. Martin, C.J. Fowler, Br. J. Pharmacol. 143 (2004) 774–784.
[54] M. Szabo, M. Agostino, D.T. Malone, E. Yuriev, B. Capuano, Bioorg. Med. Chem. Lett. 21 (2011) 6782–6787.
[55] S. Lauria, C. Perrotta, S. Casati, I. Di Renzo, R. Ottria, I. Eberini, L. Palazzolo, C. Parravicini, P. Ciuffreda, Bioorg. Med. Chem. 26 (2018) 2561–2572.
[56] R.A. Friesner, J.L. Banks, R.B. Murphy, T.A. Halgren, J.J. Klicic, D.T. Mainz, M.P. Repasky, E.H. Knoll, M. Shelley, J.K. Perry, D.E. Shaw, P. Francis, P.S. Shenkin, J. Med. Chem. 47 (2004) 1739–1749.
[57] R.A. Friesner, R.B. Murphy, M.P. Repasky, L.L. Frye, J.R. Greenwood, T.A. Halgren, P.C. Sanschagrin, D.T. Mainz, J. Med. Chem. 49 (2006) 6177–6196.
[58] T.A. Halgren, R.B. Murphy, R.A. Friesner, H.S. Beard, L.L. Frye, W.T. Pollard, J.L. Banks, J. Med. Chem. 47 (2004) 1750–1759.
[59] J.R. Greenwood, D. Calkins, A.P. Sullivan, J.C. Shelley, J. Comput. Aided Mol. Des. 24 (2010) 591–604.
[60] J.C. Shelley, A. Cholleti, L.L. Frye, J.R. Greenwood, M.R. Timlin, M. Uchimaya, J. Comput. Aided Mol. Des. 21 (2007) 681–691.